

Forecast for the remainder of the Leonid storm season.

P. Jenniskens^{1*}

The dust trails of comet 55P/Tempel-Tuttle lead to Leonid storms on Earth, threatening satellites in orbit. We present a new model that accounts in detail for the observed properties of dust tails evolved by the comet at previous oppositions. The prediction model shows the 1767-dust trail closer to Earth's orbit in 2001 than originally thought; increasing expected peak rates for North America observers. Predictions for the 2002 storms are less affected. We demonstrate that the observed shower profiles can be understood as a projection of the comet lightcurve.

¹ SETI Institute, NASA/Ames Research Center, Mail Stop 239-4, Moffett Field, CA 94035-1000

* E-mail: pjenniskens@mail.arc.nasa.gov

In the orbit of short period comets, mid-infrared images taken from satellites show a trail of dust grains that were too large to be swept into the comet dust tail by radiation pressure [1]. Those grains represent the bulk of matter lost by a comet and are thought to be responsible for the recent Leonid meteor storms on Earth. Only now has our understanding of these storms evolved enough to use the observations as a probe of comet mass loss in new and unique ways. Unlike infrared observations, grains of different masses can be measured independently and at high spatial resolution.

Dust trails are a natural consequence of the dispersion in the semi-major axis (Δa) of the orbits after ejection, causing some grains to make a wider orbit than others and return later. Recent meteor shower observations have demonstrated that the dust trails from each return of the comet are narrow and often separated, because the parent comet orbit is never the same. McNaught and Asher [2] and Lyytinen and Van Flandern [3], independently following similar work by Kondrat'eva and Reznikov [4], have estimated the location of those comet dust trails near Earth orbit by calculating the planetary perturbations on a single test particle that is ejected at perihelion with just the right difference in orbital period to end up near Earth at the time of a given shower. From year to year, the pattern of trails moves in and out of Earth's orbit, because planetary perturbations differ for particles at different positions along the comet orbit. From this, they identified the oppositions of the parent comet 55P/Tempel-Tuttle that were responsible for recent Leonid storms (Table I).

Observations of the Leonid showers have now accumulated to enough dust trail cross sections to create an accurate comet dust trail model for the ejecta of 55P/Tempel-Tuttle. This unassuming comet has an orbital period of about 33.25 years and is special only because it has passed near Earth's orbit for centuries, providing a unique historical record of Leonid storms. Many aspects of the physical interpretation of the observations are relevant to comet dust trails in general.

We measured the 1899-dust trail cross section during the 1999 Leonid Multi-Instrument Aircraft Campaign; a NASA and USAF sponsored airborne mission, while flying from Israel to the Azores [5]. The aircraft perspective enabled us to measure simultaneously intrinsically faint meteors near the zenith and intrinsically bright meteors near the horizon. We find that the smaller grains peak earlier in time and have a wider profile (Figure 1) [6]. These cross sections are well represented by a Lorentzian shape [7] as in Equation 1 (Figure

2). This is the first of a series of equations (Eq. 1-9) that will describe the dust dispersion in a trail in three dimensions. The Zenith Hourly Rate (ZHR) is a commonly used measure of number influx and is proportional to the rate of meteors observed by a visual observer under clear sky conditions [8]. W is the full-width at half maximum of the ZHR profile, while λ_0^{\max} is the time of the peak in terms of solar longitude λ_0 , which is a measure of the Earth's position in its orbit. Throughout the paper, this angle will be in Equinox J2000.0.

At the peak of the storm, the measured influx for meteoroids of visual magnitude $V < 6.5$ (or mass 2×10^{-5} g [9]) was 2.8 ± 0.4 meteoroids $\text{km}^{-2} \text{hr}^{-1}$ [10]. This corresponds [8] to a ZHR = $4,600 \pm 700 \text{ hr}^{-1}$ ($\gamma=1.0$, [8]) and an impact probability of 50% for the current satellite park as a whole. Smaller particles must have impacted in larger numbers, but did not result in satellite operation anomalies [11]. There is not a single power law over the whole mass range, as normally assumed in dust trail models [1]. The mass power index $s = 1.64 \pm 0.05$ for meteoroids of mass less than 2×10^{-3} g (+0 magnitude), while intrinsically fainter meteors have larger values, increasing to $s = 1.97 \pm 0.05$ for +6 magnitude meteors of mass 5×10^{-4} g [12]. Most of the mass is in the larger meteoroids. At least one fireball of 4 kg mass was observed from Leonid MAC, while Leonids up to 5 kg are thought to have been responsible for impacts on the Moon during the crossing of the same dust trail [13]. The distribution of impact flashes with $s = 1.6 \pm 0.1$ suggests that the size distribution is not changed at least up to 5 kg. Integrating up to this mass, the peak influx corresponds to $0.070 \text{ g km}^{-2} \text{hr}^{-1}$.

Similar Lorentz-shaped profiles are found also from the mid-infrared brightness intensity across the dust trail of comet 22P/Kopff [14]. The tail of the distribution has been interpreted as a separate dust component from grains of different size or morphology. However, the meteor shower shows no apparent change of the power law size distribution index across the Lorentz profile. We conclude that the tail of the distribution appears to be dynamically related to the peak and is not due to a separate dust component.

Three further dust trail cross sections were obtained in November 2000. The 1932- and 1866- dust trail were observed using the same intensified video cameras from a small Cessna aircraft over Florida, facilitated by Bo Gustafson of the University of Florida at Gainesville [15]. The 1733-dust trail peaked over Europe and was observed by Ilkka Yrjölä in Finland using radio forward meteor scatter to measure

the meteor rate. In Figure 3, these results are compared to visual observations collected by the International Meteor Organization [16].

These cross sections are at appropriate distances from the calculated trail centers to measure the dispersion of dust in the comet orbital plane perpendicular to Earth's orbit. Results of Lorentz profile fits are summarized in Table 1, which includes data from historic Leonid showers that originated from known trails [8]. Each shower represents a cross section at different Δa and Δr (Figure 2), and after a different number of revolutions N since epoch T . The observed rate is a product of these three factors [2], see Eq. 2: a function $f(\Delta a)$ that describes the initial dispersion along the orbit in terms of semi-major axis, a function $f_m \sim 1/N$ that describes the subsequent dispersion due to planetary perturbations and the number of revolutions (calculated from the relative distance between two nearby test particles), and a function $f(\Delta r)$ that describes the dispersion in the plane of the comet orbit in terms of radial heliocentric distance. ZHR_0 is the peak dust density in a one-revolution trail. The last two functions are derived iteratively here by plotting the observed width and peak intensity ($ZHR_0 * f(\Delta r)$ and $f(\Delta a)$, respectively) as a function of Δr and Δa . Figure 4 shows the result. The measured width W needs to be corrected for the angle $\epsilon_h = 18.1^\circ$ at which Earth crosses the trail (Eq. 3). The result, W_E , varies with Δr and is expected to be smallest at the trail center. The narrowest observed historic Leonid storms imply an intrinsic width of only $W_E^0 = 0.00013 \pm 0.00001$ AU, or $1.9 \pm 0.2 \times 10^4$ km.

The variation with Δr of peak intensity (Fig. 4a) and stream width (Fig. 4b) is skewed towards negative values of Δr for both peak intensity and width, with comparatively narrower width and larger peak activity on the sunward side of the trail. The narrowest and strongest showers are detected when the trail position is calculated to be just outside of Earth's orbit. The observed trends do not comply with a cylindrical-symmetric Lorentz-profile dust distribution (dashed lines in Fig. 4a and 4b) and is not Gaussian, as assumed in earlier models [2].

For any given functional form, there are significant discrepancies. The large deviation for the 1998 encounter with the 1899-dust trail is understood from a perturbation by Earth in the previous return of 1965 [3]. We now measure a trail displacement of $\delta r = \Delta r^{obs} - \Delta r^{cal} = 0.0031$ AU from the calculated position. Other discrepancies are more puzzling. Especially, the 1733- and 1866-dust trail encounters in 2000, which occurred at the same calculated Δr , but resulted in

significantly different peak intensity and width. The agreement is not improved by assuming that the dust density falls off (and width increases) with the number of revolutions N^2 (or N) as assumed by Lyytinen and van Flandern [3], nor with initial Δa . The latter may sound surprising, because comet dust trails do show such a behavior [1,14]. However, unlike mid-infrared images of comet dust trails, the Leonid showers are always measured near perihelion.

One important clue is that the discrepancies in peak intensity and width deviate in sync. When the trails are too dense, they also tend to be too narrow. This argues against residual effects from significant variations in the comet activity along the orbit, or from one return to the next.

We postulate that the discrepancies are due to trail shifts δr (and $\delta \lambda_0$) possibly because of the particularities of comet dust grain ejection. McNaught and Asher [2] assume simply ejection at perihelion in the direction of comet motion, while Lyytinen and van Flandern [3] assume no ejection but high radiation pressure forces to arrive at the same initial Δa . However, note that the agreement in peak time and Δr calculated may be fortuitous because these assumptions lead to the same meteoroid orbit for given Δa .

We find a smooth variation of shifts with epoch of ejection after matching a symmetric profile through the variation of peak intensity and width with Δr . The functional form that best describes the dispersion of dust in the heliocentric direction is Eq. 4 (solid line in Fig. 4a), with δr about $+0.00025$ AU. The equivalent width of this distribution (defined as integrated profile = width*peak rate) is $W_r^\circ = 0.00060 \pm 6$ AU, or $8.9 \pm 0.9 \times 10^4$ km, a factor of three larger than the equivalent width of $1.57 \times W_e^\circ = 0.00020 \pm 2$ AU in the perpendicular direction. The discrepancies from this relation are of similar magnitude and sign for ejections dating from the same epoch. There is a sinusoidal variation (Eq. 5) as a function of the year of epoch from $T = 1733$ until 1932 (solid line Figure 4c). The 1733 and 1866 trails represent the maximum and minimum of the functional trend, thus explaining the relatively large differences in shower width and intensity, despite similar Δr^{cal} .

After correcting with Eq. 5, we find that the variation of width is also described well by an exponential curve (Eq. 6), with about half the scale length. With this definition of $f(\Delta r)$ (Eq. 4+5), we can plot the corrected peak rate as a function of the initial dispersion in semi-major

axis to find a Lorentzian shaped $f(\Delta a)$ as expressed in Eq. 7, with $W_a = 0.16 \pm 0.02$ AU and $ZHR_0 = 0.6 \pm 0.1 \times 10^5$ hr⁻¹. This function represents the dispersion of dust along a one-revolution dust trail of comet 55P/Tempel-Tuttle. Note that W_a does not measure a physical distance, but rather a dispersion in semi-major axis.

The offset in the peak of the curve is an expected result from radiation pressure effects on the grains, and should be larger for smaller meteoroids. Indeed, we observe a logarithmic increase (Eq. 8) of the mass power index (s) with Δa away from the comet position (centered on magnitude +3.5 meteors).

Trail shifts can also affect the time of the peak. The peak times calculated [2,3] differ from the observed peak times by up to ± 16 -minutes, which is the same as the range in Eq. 5. Six of eight data points are fitted by Eq. 9. This completes the formalism for predicting future Leonid returns (Eq. 1-9). Results are in Table II.

Implications

Several dust trails are near Earth's orbit in November of 2001 and 2002 (Table II). Our results argue against the large dispersion and trail shifts that follow from numerical models by Brown and by Göckel and Jehn [17]. Compared to models by McNaught and Asher [2] and Lyytinen and Van Flandern [3], our predictions increase the importance of the 1767 dust trail encounter relative to that of 1866. The 1767-dust trail is now expected to give the highest peak rate for Earth-based observers, an estimated $ZHR^{\max} = 4,200$ hr⁻¹. Different solutions for δr introduce an uncertainty over the range 3,000-6,900 hr⁻¹. The 1866-dust trail will contribute only $ZHR = 2,000$ -3,500 and the 1699-dust trail 1,300-2,500 hr⁻¹. However, the latter storms are slightly wider and both will merge into a single profile with a total fluence 1.6 times higher. Earlier estimates [2,3] had this peak 4-10 times more intense. The meteors will be somewhat brighter on average than during the storm of 1999. Other strong showers are predicted for 2002, but a full Moon will illuminate this next encounter and the meteors will be fainter on average. No further storms are predicted until 2099.

The observed trail shifts (~ 0.00025 AU) are of the same order as the geostationary distance (0.00028 AU). In the anti-Sun direction, for example, the 1767-dust trail passage in 2001 causes an equivalent $ZHR = 11,000$ hr⁻¹, or about 7 particles km⁻² hr⁻¹ with mass $> 2 \times 10^{-5}$ g

at the peak. At the sunward position of geostationary orbit, the 1866- and 1699-dust trails peak at 6,800 and 4,500 hr⁻¹, respectively.

The Moon is positioned at a relatively large distance of 0.00258 AU. In 2001, the most significant impacts will occur when passing the 1833- (ZHR = 2,800 hr⁻¹) and 1800-dust trails (ZHR = 900 hr⁻¹), 2 hours after the Earth's passage by those trails at around 14 h and 16 h UT. This compares to a peak influx of about ZHR = 1,100 hr⁻¹ in 1999. Unfortunately, the Moon will be only 3 days old. In 2002, the trails will remain relatively far from the Moon.

Discussion

The shower profiles (Figs. 1 and 3) can be understood as a projection of the comet's light curve. Let us assume that the dust production rate is proportional to the water production rate. The lightcurve of comet 55P/Tempel-Tuttle during the 1998 return is well described by [18] $m_r = 7.5 + 35 \log r$ (AU) (-100 to -40 days before perihelion) and $m_r = 8.5 + 20 \log r$ (-40 days to + 100 days after perihelion), with heliocentric magnitude $m_r = m_1 - 5 \log d$ (AU). 90% of all ejection occurs within 60 days from perihelion. Also, the water production rate of comets, as observed by OH radio line observations, correlates well with m_r , without invoking additional corrections to the OH line intensity or the visual magnitude: $\log Q_{\text{H}_2\text{O}}(r)$ [mol/s] = $30.74 \pm 0.02 - 0.240 \pm 0.03 m_r$ (magn.) [19].

Most of the dust ejected at heliocentric distance r will end up near perihelion (where Earth encounters the stream) having dispersed away from the comet orbit to a distance Δx perpendicular to the comet orbital plane: $\Delta x = V_{ej} \perp(r) \Delta t(r)$. The function $\Delta t(r)$ is the time lapse from ejection until perihelion, and is readily derived from the comet ephemeris. By making the usual assumption that the ejection velocity is proportional to a power of the heliocentric distance, we can transform $Q(r)$ into $Q(\Delta x)$ as a representation of the dust dispersion perpendicular to the orbital plane and, after correction for projection, in the path of the Earth.

The time-independent ZHR profile width can be understood because each particle, to first order, will return to its point of ejection after one return. Thus, the width measured near perihelion reflects the heliocentric dependence on ejection velocities and does not necessarily increase with orbital period.

The ejection velocities are determined by the width of the curve near the peak, while the tail of the Lorentz profile is sensitive to the adopted power law for the heliocentric distance dependence. To get particles far from the stream center as observed in the Lorentz wings of the ZHR profile, one has to invoke an increase of the ejection velocity with heliocentric distance. Within the range of comet activity, a perfect fit is provided to the intrinsic Lorentzian shape of the dust density in Earth's path (with $W_E = 0.00013$ AU) for:

$$\text{Log } V_{ej}^{\perp} \text{ (m/s)} = -0.22 \pm 0.05 - 0.19 \pm 0.03 \log M \text{ (g)} + 1.27 \pm 0.05 \log r \text{ (AU)} \quad (10)$$

The actual ejection velocity includes the comet's escape velocity, which is about 1.4 m/s for a comet radius $R_c = 1.9$ km [20]. Hence, $V_{ej}^{\perp} = 3.0 \pm 0.3$ m/s at perihelion for 3×10^{-4} g particles (+3.5 magn.). The reported mass dependence of ejection in Eq. 10 follows from the variation of width with mass (Fig. 1). The model provides a natural explanation for the dispersion of particles in the profile and the implication is that the meteoroids in the ZHR profile tails were ejected at relatively large heliocentric distance.

In contrast, the measured ejection velocities are an order of magnitude smaller than predicted by the Whipple model for water vapor drag of cometary dust grains, modified to include adiabatic expansion, blackbody-limited nucleus temperature, and distributed production throughout the coma for ejection at perihelion, and specifically for particle density $\rho \sim 0.7$ g/cm³ [22] and $R_c = 1.9$ km [21]:

$$\text{Log } V_{ej} \text{ (m/s)} = 1.05 \pm 0.33 - 0.167 \log M \text{ (g)} - 0.60 \log r \text{ (AU)} \quad (11)$$

The predicted speed for a 3×10^{-4} g meteoroid is $V_{ej} = 44$ m/s (within factor of 2). The large tolerance reflects the various versions of Eq. 11 that are in use. If the dust ejection velocity is proportional to the gas ejection velocity (Eq. 11), the result does not show the Lorentz wings in the observed ZHR curves.

One way to reconcile the Whipple model is to consider directional ejection from a dust jet and only the component of the mean ejection velocity vector perpendicular to the comet orbital plane. Indeed, a dust jet was observed 1 month prior to the 1998 perihelion passage of comet 55P/Tempel-Tuttle, with an amplitude of 25° centered on a north-north-eastern direction [23]. The amplitude of the jet motion

suggests a hot spot at +65° N, and a rotation period of 15.33±0.02 hr [23].

The observed trail displacements (Fig. 4c) and the mass dependent shift in the node (Fig. 1) can be understood as an effect of such jet. Ejection in a northerly direction explains the negative displacement in node. The torque exerted by the jet will cause a precession of the spin axis that can qualitatively account for the observed radial displacement δr with a semi-period of 270±80 years (Eq. 5), and in $\delta\lambda_0$ with a semi-period of 180±20 years (Eq. 9), by changing the mean direction of ejection at perihelion in each return. With a nuclear axis ratio larger than 1.5 [20], this motion is not necessary a simple sine law, hence the different semi-periodicities.

Directional ejection can account for the lack of a Lorentz wing in the observed $f(\Delta r)$. This is because the ejection vector in the comet orbital plane will be mostly in the direction of comet motion at large heliocentric distances, while nearly perpendicular to the comet motion vector at perihelion. The effect is to suppress the Lorentz wings. The 3 times higher dispersion implies that the ejection velocity at perihelion is $V_{ej} = 9.1 \pm 1.8$ m/s, still short of the Whipple speed (Eq. 11).

Directional ejection has the opposite effect on the distribution of dust in the comet orbit $f(\Delta a)$. However, ejection in the direction of motion can not account for the full observed dispersion with Δa . Instead, a dispersion in perihelion distance Δq does give the correct fall off away from the comet if Δq is related to a difference in semi-major axis (Δa) relative to that of the comet according to:

$$\Delta a = - (1+e)^{-1} G M (1-\beta) / (V_q^2/2 - GM (1-\beta)/(q \pm \Delta q)) + (1+e)^{-1} G M / (V_q^2/2 - GM/q) \quad (12)$$

where e is the orbit eccentricity: $q = a(1-e)$. A good fit to the data (solid line in Fig. 4d) follows by plotting $Q(\Delta x)$ versus $\langle \Delta a \rangle$, a mean of the two alternative possibilities of $\pm \Delta q$. For the comet velocity at perihelion $V_q = 41,600$ m/s and $q = 0.9766$ AU, the variation in Figure 4d is matched for $\Delta q = 6.2 \pm 0.7 * \Delta x$ and $\beta = 7.0 \pm 0.6 \times 10^{-4}$. The model predicts the decay of dust density in front of the comet, where no data are available.

The parameter β in Eq. 12 is the ratio of radiation over gravitational forces. While most of the observed dispersion is understood in terms

of ejection velocities, the effect of radiation pressure is to shift the $f(\Delta a)$ profile to longer Δa due to an effective decrease of the gravitational potential. Unlike ejection velocities, the main effect will be along the comet orbit. The value derived from the observed shift of the peak δa is valid for a visual magnitude +3.5 Leonid meteor of initial mass 3×10^{-4} g (Eq. 2). From the common equation for β [24], we conclude that the average meteoroid density is $\rho = 0.97 \pm 0.13$ g/cm³, if the radiation pressure coefficient $\langle Q_{pr} \rangle = 1$ and the grains are spherical in shape. This compares well to the estimate of $\rho \sim 0.7$ g/cm³ from the deceleration of a Leonid fireball [22].

To reconcile the observed ejection speed and its increase with heliocentric distance with the Whipple model, we postulate that larger grains fall apart in the comet coma and are the main source of the smaller grains. Such a scenario is not unlikely given that most of the mass is locked up in the larger grains. In that case, the ejection velocities of smaller grains reflect mostly those of the larger meteoroids, because gas drag is not efficient far from the nucleus surface. In order to explain the increasing speed with Δr , grains of given mass need to be derived from on average larger meteoroids closer to the Sun. Such an effect could occur because of increased thermal stresses on the grains. Indeed, the large grain mass distribution agrees with the value of $s = 1.53 \pm 0.1$ (reportedly valid over a wide 10^{-12} to 10^{-3} kg mass range) near the nucleus of comet 1P/Halley and expected to reflect the dust distribution shortly after ejection [25]. The mass distribution for small grains is consistent with that expected for catastrophic fragmentation, where $\Delta N(M) \cdot M \sim M^{+k/3} \Delta(\log M)$, with $k=0.6$ for diameters smaller than one-tenth the diameter of the original mass [26]. Dust fragmentation in the comet coma is frequently implied to account for dust distributions and comet dust tail striae. Our meteor observations, too, show tentative evidence for spatial and temporal correlations that suggest breakup more than one return before Earth's encounter [27].

We now have all parameters in hand to calculate the total dust mass loss of 55P/Tempel-Tuttle during one return. That mass is proportional to the equivalent dimensions of the dust trail: W_r° by $1.57 \times W_E^\circ$ by $1.57 \times ((a+W_a)^{1.5} - a^{1.5})$ yr., and the peak dust density derived from: $ZHR_0 = 0.6 \pm 0.1 \times 10^5$ hr⁻¹, while $ZHR = 4,600$ hr⁻¹ corresponds 0.070 g km⁻² hr⁻¹ integrated up to $M = 5$ kg. From this, we calculate a total dust mass loss for each return of comet 55P/Tempel-Tuttle of $2.6 \pm 0.7 \times 10^{10}$ kg. From the observed visible magnitude light curve of comet 55P/Tempel-Tuttle we derive a total water production loss of

References and notes:

- [1] Davies, J.K., Sykes, M.V., Reach, W.T., Boulanger, F., Sibille, F., Cesarsky, C.J., 1997, *Icarus*, 127, 251-254; Reach, W.T., Sykes, M.V., Lien, D., and Davies, J.K., 2000, *Icarus*, 148, 80-94; Fulle, M., 2000, *Icarus* 145, 239-251; Fulle, M., Colangeli, L., Mennella, V., Rotundi, A., and Bussoletti, E., 1997, *A&A Suppl. Ser.*, 126, 183-195. Epifani, E., Colangeli, L., Fulle, M., Brucato, J.R., Bussoletti, E., de Sanctis, M.C., Mennella, V., Palumba, E., Palumbo, P., and Rotundi, A., 2001, *Icarus*, 149, 339-350;
- [2] McNaught, R.H., Asher, D.J., 1999, *WGN, Journal of the IMO*, 27, 85-102; McNaught, R., Asher, D., 2000, Update on website: <http://www.arm.ac.uk/leonid/encounters.html>
- [3] Lyytinen, E., 1999, *Meta Research Bulletin*, 8, 33-40; Lyytinen E., van Flandern T., 2000, *Earth, Moon and Planets*, 82-83, 149-166.
- [4] Kondrat'eva, E.D., Reznikov, E.A., 1985, *Sol. Syst. Res.*, 19, 96-101.
- [5] Jenniskens, P., Butow S.J., and Fonda, M., 2000, *Earth, Moon and Planets*, 82-83, 1-26; Vizard F., 1998, *Meteor Mission, Popular Science* (Nov. issue), p. 68; See also: <http://leonid.arc.nasa.gov>.
- [6] The full-width-at-half-maximum is $W = 0.037 \pm 0.001^\circ$ for the 2×10^{-3} g meteoroids seen near the horizon ($\lambda_0 = 235.284 \pm 0.001^\circ$), $W = 0.046 \pm 0.004^\circ$ for the 6×10^{-4} g meteoroids seen higher up in the sky with similar instruments ($\lambda_0 = 235.274 \pm 0.002^\circ$), and $W = 0.056 \pm 0.003^\circ$ for the 5×10^{-4} g particles measured in the zenith with high-definition TV cameras ($\lambda_0 = 235.275 \pm 0.001^\circ$) [28]. Incidentally, this trend is consistent with the displaced profile of the 0.2-2.5 kHz ELF/VLF detection of meteors reported by C. Price and M. Blum (2000, *Earth, Moon and Planets*, 82-83, 545-554). We derive a width of $W = 0.080 \pm 0.008^\circ$ and a peak time $\lambda_0 = 235.269 \pm 0.005$, suggesting meteoroids of mass $\sim 3 \times 10^{-5}$ g (diameter 200 micron).
- [7] Jenniskens, P., Crawford, C., Butow, S., Nugent, D., Koop, M., Holman, D., Houston, K., Kronk, G., Beatty, K., 2000, *Earth, Moon and Planets*, 82-83, 191-208.

[8] Jenniskens, P., 1995. *Astron. Astrophys.*, 295, 206-235.
Jenniskens, P., Betlem, H., 2000, *Astrophys. J.*, 531, 1161-1167.

[9] Throughout the paper, we will use the empirical mass-luminosity relationship [12]: $\log M(g) = -1.98(\pm 0.02) - 0.43(\pm 0.01)m_v - 0.07(\pm 0.26)/\log(\cos z)$ with m_v the peak visual magnitude for a distance of 100 km, and z the zenith angle of impact (47° at the time of the peak).

[10] Holman, D., Jenniskens, P., 2001, *WGN, the Journal of IMO*, 29, 77-84.

[11] Treu, M.H., Worden, S.P., Bedard, M.G., Bartlett, R.K., 2000, *Earth Moon and Planets*, 82-83, 27-38. [1] Beech, M., Brown, P., and Jones, J., 1995, *Q.J.R. Astr. Soc.*, 36, 127-152; McBride, N., McDonnell, J.A.M., 1998, *Plan. Space Sci.*, 47, 1005-1013; Treu, M.H., Worden, S.P., Bedard, M.G., Bartlett, R.K., 2000, *Earth Moon and Planets*, 82-83, 27-38.

[12] Brown, P., Campbell, M.D., Ellis, K.J., Hawkes, R.L., et al., 2000, *Earth, Moon and Planets*, 82-83, 167-190. Arlt, R., Bellot Rubio L., Brown, P., Gijssens, M., 1999, *WGN, Journal of the IMO*, 27, 286-295.

[13] Bellot-Rubio, L.R., Ortiz, J.L., Sada, P.V., 2000, *Earth, Moon and Planets*, 82-83, 575-598.

[14] Davies, J.K., Sykes, M.V., Reach, W.T., Boulanger, F., Sibille, F., Cesarsky, C.J., 1997, *Icarus* 127, 251-254.

[15] Jenniskens, P., Gustafson, B. Å. S., 2000, *WGN, Journal of the IMO*, 28, 209-211.

[16] Arlt R., Gijssens M., 2000, *WGN, the Journal of the IMO*, 28, 195-208.

[17] Brown, P.G., 2000, *Evolution of Two Periodic Meteoroid Streams: the Perseids and Leonids*, Thesis (PHD). THE UNIVERSITY OF WESTERN ONTARIO (London, CANADA), 286 pp.; Cooke B., 2001, "The April (T-7) Leonid forecast for 2001", Updated in "The July Leonid forecast for 2001 (Applicable to Earth and Spacecraft in LEO)", Marshall Space Flight Center internal document, distributed electronically; Göckel, C.; Jehn, R., 2000, *MNRAS*, 317, L1-L5;

Table 1: Dust trail parameters from past Leonid outbursts.

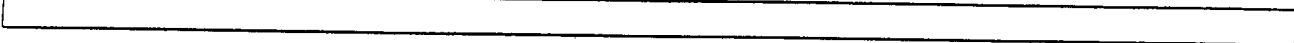
Year	N*	Trail*	f_m	Δa	Δr	δr_{obs}	W_{obs}	W_{cal}	ZR_{obs}	ZR_{cal}	S_{obs}
1999	3	1899	0.38	0.138	-0.00066	+0.00020	0.00063±3	0.00073	4,600±700	4,593	1.89
1998	3	1899	0.40	0.050	+0.00440	-0.0031	0.0024±7	0.22	70±20	0	1.64
1999	4	1866	0.50	0.118	+0.00160	+0.00003	0.0049±15	0.0039	30±15	109	1.83
2000	4	1866	0.13	0.114	+0.00077	-0.00013	0.0014±2	0.0012	390±20	459	1.76
2000	2	1932	0.55	0.300	-0.00120	+0.00028	0.0014±2	0.0013	255±20	312	1.99
2000	8	1733	0.27	0.064	+0.00076	+0.00039	0.0025±6	0.0020	230±20	216	1.77
1969	1	1932	0.95	0.934	-0.00004	+0.00037	0.00052±9	0.00059	180±20	192	2.19
1966	2	1899	0.52	0.168	-0.00013	+0.00028	0.00049±5	0.00043	14,000±3,000	17,926	1.99
1867	1	1833	1.00	0.373	-0.00014	+0.00006	0.00042±7	0.00043	4,300±900	4,105	--
1866	4	1733	0.37	0.059	-0.00029	+0.00051	0.00058±11	0.00046	6,800±1,100	9,145	--
1833	1	1799	0.95	0.174	-0.00021	+0.00021	--	0.00042	-50,000	31,416	--

*) calculations from [2, 3]

Table 2: Forecast for the 2001+2002 encounters.

N	Year	λ_{max} (J2000)	Time (UT)	W (AU)	FWHM (hr)	ZHR ^{max} (hr ⁻¹)	s	Lyytinen [3]	Asher [2]	Brown [*] [17]	Time [2,3]
<i>Nov. 17, 2001 (UT)</i>											
1	(1965)	235.24	13:14	0.017	--	0	2.16	--	--	--	--
2	(1932)	235.37	16:20	0.030	--	0	2.04	--	--	--	--
3	(1899)	235.54	20:22	--	--	0	1.97	--	--	--	--
<i>Nov. 18, 2001 (UT)</i>											
8	(1733)	236.12	10:10	--	--	0	1.71	--	--	--	--
7	(1767)	236.119	10:09	0.00047	0.66	4,200	1.76	2,000	2,500?	100	09:58
6	(1800)	236.202	12:07	0.0030	4.25	40	1.76	110	--	1,300	12:00
5	(1833)	236.279	13:57	0.0049	6.80	14	1.79	60	--	--	14:10
10	(1667)	236.408	17:01	0.00147	2.05	170	1.59	600	--	(" incl)	17:22
11	(1633)	236.422	17:21	0.00091	1.26	510	1.56	260	--	(" incl)	17:55
9	(1699)	236.413	17:08	0.00088	1.23	1,800	1.64	2,000	9,000	600	17:31
4	(1866)	236.446	17:55	0.00058	0.81	2,700	1.86	6,100	15,000	200	18:22
<i>Nov. 17, 2002 (UT)</i>											
1	(1965)	235.29	20:35	0.0060	--	0	2.19	--	--	--	--
<i>Nov. 18, 2002 (UT)</i>											
2	(1932)	--	--	--	--	0	2.07	--	--	--	--
3	(1899)	235.75	07:31	--	--	0	2.00	--	--	--	--
<i>Nov. 19, 2002 (UT)</i>											
7	(1767)	236.615	04:07	0.00047	0.65	4,900	1.82	4,500	15,000	--	04:02
6	(1800)	236.710	06:23	0.0028	3.96	58	1.83	--	--	--	06:23
5	(1833)	236.709	06:22	0.0032	4.49	41	1.83	160	--	--	06:45
4	(1866)	236.871	10:13	0.00040	0.56	5,700	1.90	7,400	30,000	--	10:44
<i>Nov. 19, 2006 (UT)</i>											
2	(1932)	236.620	04:53	0.00055	0.77	120	2.20	50	100	--	04:48
<i>Nov. 18, 2007 (UT)</i>											
	(1932)	236.109	22:51	0.00042	0.58	200	2.22	30	--	--	22:55

* Low rates due to assumed large dispersion



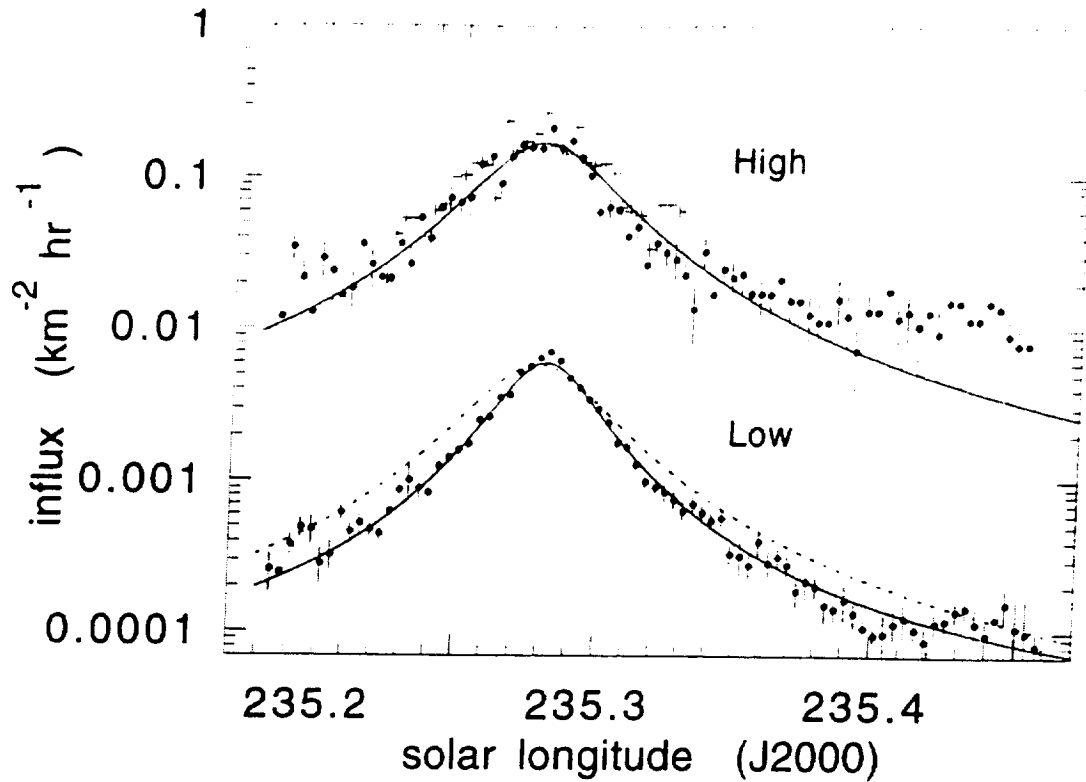


Fig. 1.: 1999 Leonid storm influx profiles measured by cameras pointed at 37° (high) and 21° (low) elevation from the aircraft window. They represent masses of 5×10^{-4} g and 2×10^{-3} g, respectively. Data from the intensified High-Definition TV camera at 90° elevation [29] are shown as crosses. To facilitate comparison, the dashed line copies the Lorentz curve fit for the high cameras to match the peak of the low cameras. The activity curves are scaled to match the cumulative influx up to the given mass that was representative of each set of observations. No smoothing applied. Error bars represent the statistical error from the number of meteors in each interval.

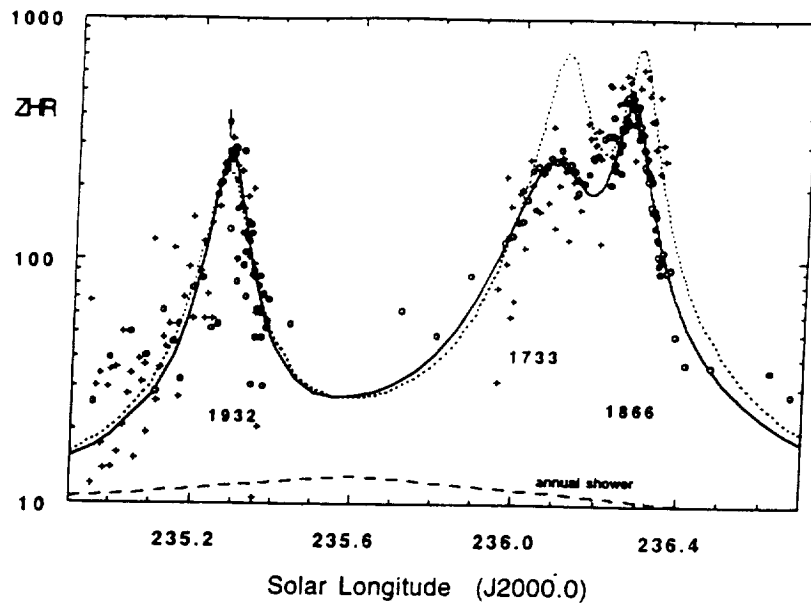


Fig. 3.: Zenith Hourly Rate curves for the 2000 encounters with the 1932-, 1733-, and 1866-dust trails. Black dots are results from intensified video cameras, while crosses are radio-MS data. Open circles are visual observations reported in Arlt and Gijssens [16]. The solid line is a fit of Lorentzian profiles. The broad dashed line is the level of annual shower activity in non-outburst years. The narrow dashed line shows the predicted rate by Lytinen and Van Flandern [3].

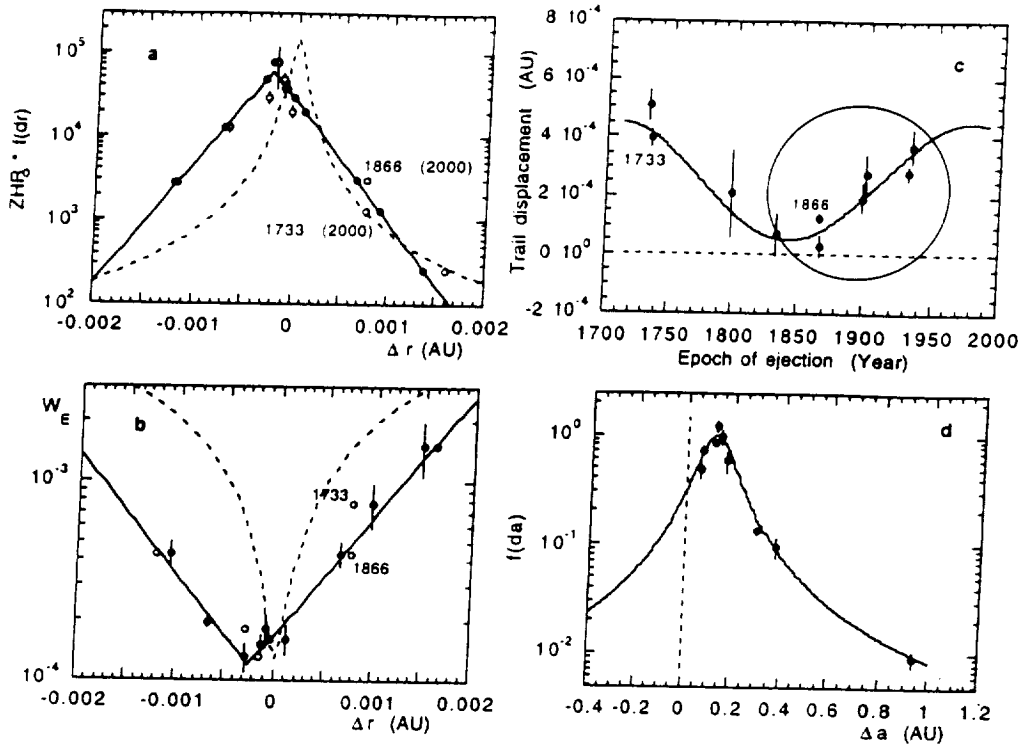


Fig. 4a: Trail cross section along a radial direction to the Sun. Open symbols are observed values, dark symbols show values after correcting for trail shifts of Fig. 4c. **4b:** As Fig. 4a, for the variation of shower width with heliocentric distance. **4c:** Trail shifts that would fit the observed flux to a smooth exponential behavior (dark symbols in fig. 4a). The open circle shows one trail equivalent width. **4d:** Variation of trail dust density with intrinsic semi-major axis dispersion (variation along the comet orbit) after correction for trail shifts in Fig. 4c.